Journal of Solid State Chemistry **165,** 266–277 (2002)
doi:10.1006/jssc.2002.9520, available online at http://www.idealibrary.com on IDEAL®

Synthesis, Crystal, and Magnetic Structures of the Sodium Ferrate (IV) Na_4FeO_4 Studied by Neutron Diffraction and Mössbauer Techniques

C. Jeannot,* B. Malaman,* R. Gérardin,*,[1] and B. Oulladiaf†

* *Laboratoire de Chimie du Solide Minéral, Université Henri Poincaré-Nancy 1, associé au CNRS (UMR 7555), B.P. 239, 54506 Vandoeuvre-les-Nancy Cedex, France; and † Institut Laue-Langevin, B.P. 156, 38042 Grenoble Cedex 9, France*

Received October 12, 2001; in revised form January 22, 2002; accepted January 25, 2002; published online March 22, 2002

The alkali sodium ferrate (IV) Na_4FeO_4 has been prepared by solid-state reaction of sodium peroxide Na_2O_2 and wustite $Fe_{1-x}O$, in a molar ratio Na/Fe=4, at 400°C under vacuum. Powder X-ray and neutron diffraction studies indicate that Na_4FeO_4 crystallizes in the triclinic system $P\bar{1}$ with the cell parameters: a=8.4810(2) Å, b=5.7688(1) Å, c=6.5622(1) Å, α=124.662(2)°, β=98.848(2)°, γ=101.761(2)° and Z=2. Na_4FeO_4 is isotypic with the other known phases Na_4MO_4 (M=Ti, Cr, Mn, Co and Ge, Sn, Pb). The solid solution $Na_4Fe_xCo_{1-x}O_4$ exists for x=0–1 and we have followed the evolution of the cell parameters with x to determine the lattice parameters of the triclinic cell of Na_4FeO_4. A three-dimensional network of isolated FeO_4 tetrahedra connected by Na atoms characterizes the structure. This compound is antiferromagnetic below T_N=16 K. At 2 K the magnetic cell is twice the nuclear cell and the magnetic structure is collinear (μ_{Fe}=3.36(12) μ_B at 2 K). This black compound is highly hygroscopic. In water or on contact with the atmospheric moisture it is disproportionated in Fe^{3+} and Fe^{6+}. The Mössbauer spectra of Na_4FeO_4 are fitted with one doublet (δ=−0.22 mm/s, Δ=0.41 mm/s at 295 K) in the paramagnetic state and with a sextet at 8 K. These parameters characterize Fe^{4+} high-spin in tetrahedral FeO_4 coordination.

Key Words: **sodium ferrate(IV); crystal structure; neutron diffraction; magnetic structure; ^{57}Fe Mössbauer spectroscopy.**

INTRODUCTION

In the Na–Fe–O system, a great number of compounds have been reported in the literature (1–15) as Fig. 1 shows and we see that the basicity of the sodium ferrates allows the iron to adopt multiple oxidation states: II, III, IV, V and VI. Nevertheless, it remains that the sodium ferrate(III) family is the richest. The other compounds are rather unusual but, thanks to their potential oxidizing properties, they can find useful applications in the environmental domain.

In 1956, Scholder *et al.* (9) have disclosed the existence of Na_4FeO_4, synthesized by annealing a mixture of sodium oxide Na_2O and Fe_2O_3 for 30 min at 150°C and 1 h at 450°C, under a stream of, dried and carbon dioxide free, oxygen. Neither physical properties nor structural characterization are reported and the authors only noted that Na_4FeO_4 is extremely hygroscopic and quickly decomposes in air.

In 1958, Harrison and Toole (10), working on the reaction between alkali metal ferrate (III) and alkali metal compound (the alkali metal may be the same or different than that present in the alkali metal ferrate(III)) in the presence of oxygen between 300 to 500°C, have patented the synthesis of disodiumferrate(IV) Na_2FeO_3. In 1987, Kiselev *et al.* (11) have synthesized Na_2FeO_3 by reaction of Fe_2O_3 with freshly prepared Na_2O_2 in a stream of dried oxygen at 400°C, for 24 h. In 1996, Kopelev (16), in a compilation of Mössbauer data of alkali metal ferrate (IV)–(VI), did not notice any comprehensive study of Na_4FeO_4.

Thus, up to now, only two sodium ferrates(IV) have been clearly identified, Na_2FeO_3 and Na_4FeO_4, but their structural and physical properties remain unexplored. This can be explained by the difficulty to synthesize pure samples and by their high reactivity with water vapor.

In the course of a systematic investigation of new non-toxic oxidizing agents for the treatment of used water, we came across the Na–Fe–O system. In this paper, we propose a novel way of synthesis for pure tetrasodium ferrate(IV) Na_4FeO_4 and we report on its structural and magnetic properties by means of powder X-ray diffraction, bulk magnetization, powder neutron diffraction and Mössbauer spectroscopy measurements. The chemical reactivity of Na_4FeO_4 is also analyzed.

EXPERIMENTAL

The samples were prepared from a mixture of sodium peroxide Na_2O_2 and iron oxide $Fe_{1-x}O$ with various Na/Fe molar ratios. These mixtures, confined in silver crucibles, were sealed inside evacuated "Pyrex" ampoules and heated at 400°C for 15 h.

[1]To whom correspondence should be addressed. E-mail: rene.gerardin@lcsm.uhp-nancy.fr.

0022-4596/02 $35.00

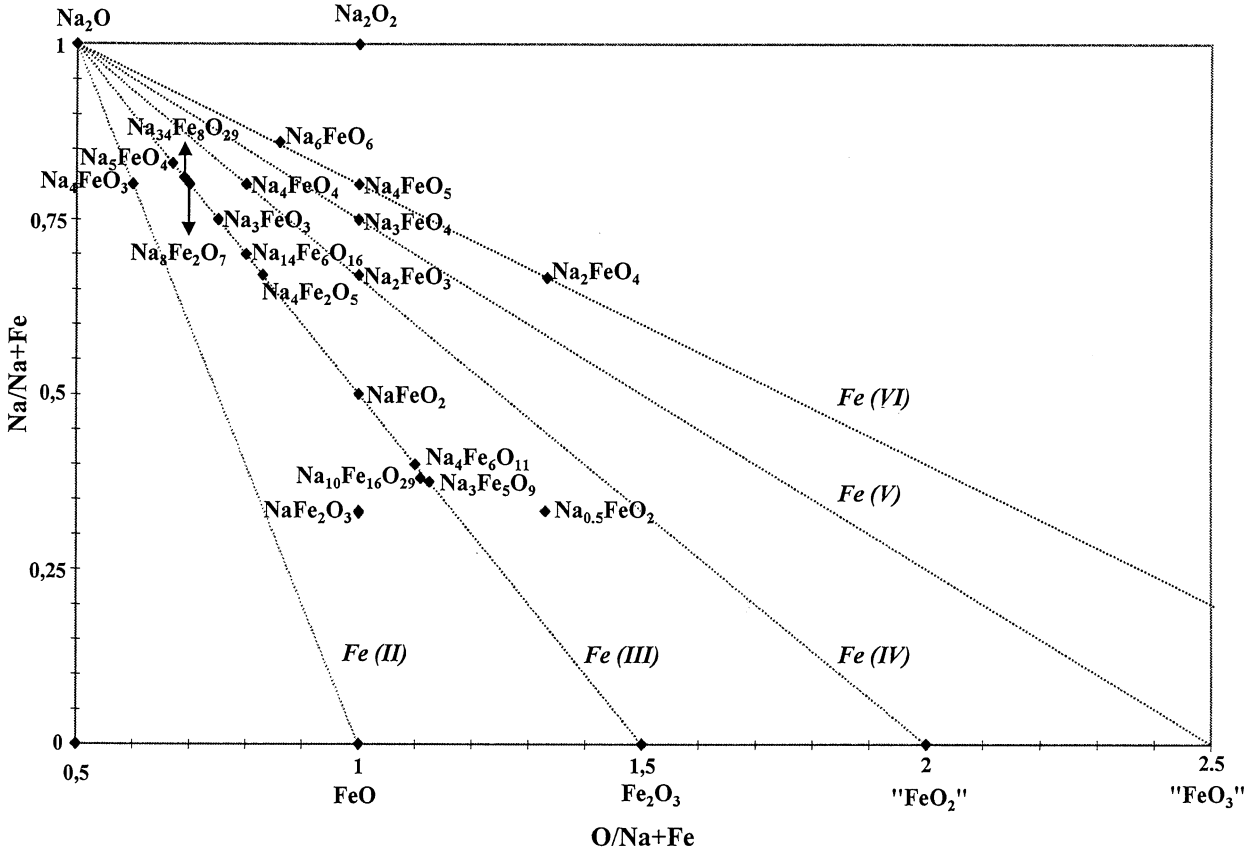

FIG. 1. Sodium ferrates previously reported.

The starting material $Fe_{1-x}O$ was prepared by reduction of Fe_2O_3 at 600°C in an appropriate H_2/H_2O atmosphere while Na_2O_2 is a commercial reagent without further purification. As Na_2O_2 and Na_4FeO_4 are very hygroscopic, all handlings were carried out in an air dried glove box in the presence of diphosphoruspentoxide P_2O_5.

The purity of the samples and the cell parameters of the phases were studied by powder X-ray analysis (Guinier Co$K\alpha$). Powders were embedded between two "Mylar" sheets to avoid contact with the air.

Magnetic measurements were performed (between 298 and 4.2 K), on a MANICS magneto-susceptometer in a magnetic field of up to 1.6 T.

Neutron diffraction experiments were carried out on powder samples at the Institut Laue Langevin, Grenoble. Several diffraction patterns were recorded, in the temperature range 300–1.6 K, with the double-axis multicounter diffractometers D1b and D2b using neutron wavelengths of 2.524 and 2.400 Å, respectively. The analysis of the patterns was performed by the Rietveld profile refinements (17) using the software FULLPROF (18). In such an experiment, the sample is kept in an airtight vanadium sample holder, filled in the glove box to prevent contact with atmospheric moisture.

The Mössbauer spectra were collected with a conventional constant acceleration spectrometer with 1024 channels. The absorber is placed in a special holder that prevents contact with the atmosphere. Isomer shifts are reported with respect to α-iron at room temperature. The Mössbauer effect data were analyzed by using least-squares fitting minimization techniques (19) to evaluate the hyperfine spectral parameters.

SYNTHESIS AND CRYSTAL STRUCTURE

Synthesis

X-ray powder diffraction patterns of mixtures with initial molar ratios Na/Fe < 4 show the coexistence of two phases: Na_4FeO_4 and the sodium ferrate(III) $NaFeO_2$, whereas for Na/Fe > 4 the products are mixtures of Na_4FeO_4 and an excess of Na_2O_2.

Thus, single-phase sodium ferrate(IV) sample is only observed for a molar ratio Na/Fe strictly $= 4$. The corresponding powder sample is black. It may be noted that similar pure samples can also be prepared using various starting iron compounds such as Fe_2O_3, Fe_3O_4 or $NaFeO_2$. Moreover, it is noteworthy that annealing duration > 24 h lead

to final products that contain sodium ferrate(III) $NaFeO_2$ besides the Na_4FeO_4 compound.

Chemical analysis. The oxidation state of the iron has been determined by chemical analysis according to the following redox procedure.

A known quantity of Na_4FeO_4 sample (Na/Fe = 4 initial ratio) was dissolved in a known excess of titrated Fe^{2+} solution (Mohr salt). After reaction ($Fe^{4+} + Fe^{2+} \rightarrow 2\ Fe^{3+}$), the excess of Fe^{2+} ions is determined by $K_2Cr_2O_7$ titration in sulfuric acid medium. For all the tests carried out, we have always found a molar ratio $Fe^{4+}/Fe^{2+} = 1$ (known by the weight of Na_4FeO_4 used)/Fe^{2+} (consumed during the oxidation–reduction reaction).

This chemical analysis clearly confirms that our samples (Na/Fe = 4) are pure and that iron is at the (IV) oxidation state.

Structure Determination

All attempts to produce single crystals have failed and the crystal study has been undertaken by using powder X-ray and neutron diffraction techniques.

X-ray diffraction study. Crystallographic investigations on the ternary compounds of general formula A_4MO_4 (20) have shown that the compounds Na_4MO_4 (M = Ti, Cr, Mn, Co and Si, Ge, Sn, Pb) and K_4MO_4 (M = Ti, Zr, Hf, Cr, Mn and Ge, Sn, Pb) are isotypic and crystallize in the triclinic symmetry. It is worth noting the absence of vanadate and ferrate in these series. The various cell parameter values observed along these two families are given in Table1.

More recently, the crystal structures of Na_4TiO_4 (21), Na_4CrO_4 (22) and Na_4CoO_4 (23) have been determined on single crystals. The two former compounds crystallize in the $P-1$ space group whereas Na_4CoO_4 crystallizes in the non-centric space group $P1$. Table 2 allows a comparison between the atomic positions of the different atoms in Na_4CrO_4 ($P-1$) and in Na_4CoO_4 ($P1$). In the latter compound, the lowering of symmetry yields atomic positions that can be associated in pairs of atoms with coordinates very close to centro-symmetric values ($\Delta = \pm 5 \times 10^{-3}$).

Bearing these observations in mind, one can conclude that the three compounds are, in first approximation, isostructural and characterized by a three-dimensional arrangement of isolated TO_4 tetrahedra. The TiO_4 and CrO_4 tetrahedra are rather regular (Ti–O = 1.826–1.836 Å, Cr–O = 1.740–1.776 Å) whereas the CoO_4 tetrahedra are slightly distorted (Co–O = 1.76–1.85 Å).

In order to determine the crystal system and the cell of Na_4FeO_4, we show at first that Na_4FeO_4 is isotypic with Na_4CoO_4 in showing, by the synthesis, that the $Na_4Fe_xCo_{1-x}O_4$ (x = 0–1) phases form a continuous solid solution. These phases, which are all hygroscopic, were prepared by annealing mixtures of [$Na_2O_2 + xFe_{1-x}O + (1-x)$ CoO], in the molar ratio $Na/(Fe + Co) = \frac{4}{1}$, at 400°C for 12 h, under vacuum. Indeed, the powder diagrams recorded on Guinier camera (Fig. 2) show only one triclinic phase for each composition. Taking the $Na_4Co_1O_4$ X-ray diffraction pattern as a starting point (23), we have refined, step by step, the cell parameters of the $Na_4Fe_xCo_{1-x}O_4$ phases for x = 0, 0.25, 0.30, 0.50, 0.60, 0.80 and 1 (Table 3). The Na_4FeO_4 unit cell dimensions so obtained are:

$$a = 8.48(1)\ \text{Å}, \qquad \alpha = 124.7(1)^\circ,$$
$$b = 5.76(1)\ \text{Å}, \qquad \beta = 98.9\ (3)^\circ,$$
$$c = 6.56(1)\ \text{Å}, \qquad \gamma = 101.8(3)^\circ.$$

As shown in Fig. 2, the "Mylar" sheets holder, used to avoid contact between the sample and the atmospheric moisture, leads to X-ray patterns having a strong background and two proper large diffraction peaks. Thus, in order to refine the crystal structure of Na_4FeO_4, we have decided to use neutron diffraction technique.

Neutron diffraction study. A first neutron diffraction experiment has been carried out on D1b spectrometer at 295 K (Fig. 3a) but, in order to obtain accurate results, a second neutron diffraction experiment has been carried out on D2b (Fig. 3b) using the wavelengths of 2.524 and 2.400 Å, respectively. The step increment of the diffraction angle 2θ is 0.200 for the D1b data and 0.050 for the D2b data.

The two patterns (Fig. 3) confirm the conclusions deduced from the above X-ray study. The weak unindexed peak near 25° on D1b originates from the sodium hydroxide hydrate impurity and the peak at 72° arises from the V sample holder.

TABLE 1
Ranges of Triclinic Cell Parameters Observed (20) in: Na_4MO_4 (M=Ti, Cr, Mn, Co and Si, Ge, Sn, Pb) K_4MO_4 (M=Ti, Zr, Hf, Cr, Mn and Ge, Sn, Pb)

	a (Å)	b (Å)	c (Å)	α (°)	β (°)	γ (°)	V (Å^3)
Na_4MO_4	5.71–5.99	8.54–8.95	6.34–6.66	98.21–99.45	123.33–124.19	98.58–99.43	243.80–279.78
K_4MO_4	6.32–6.58	9.54–9.94	6.90–7.28	103.87–104.25	122.97–123.51	94.81–95.42	323.98–369.45

TABLE 2
Atomic Coordinates for Na_4CrO_4 $P-1$ (22) and Na_4CoO_4 $P1$[a] (23)

Na_4CrO_4				Na_4CoO_4			
Atom	x	y	z	Atom	x	y	z
Cr	0.2460	0.5660	0.8453	Co(11)	0.2460	0.4360	0.1563
				Co(12)	− 0.2460	− 0.4360	− 0.1563
Na(1)	− 0.4345	− 0.2123	0.5191	Na(11)	− 0.4351	− 0.2063	0.5189
				Na(12)	0.4262	0.2169	− 0.5222
Na(2)	− 0.0160	0.0088	0.7613	Na(21)	− 0.0146	− 0.0017	0.7565
				Na(22)	0.0135	− 0.0345	− 0.7719
Na(3)	− 0.1763	0.3372	− 0.4011	Na(31)	0.1727	− 0.3444	0.4130
				Na(32)	− 0.1813	0.3407	− 0.3960
Na(4)	− 0.6058	0.1871	− 0.0503	Na(41)	− 0.6082	0.1848	− 0.0482
				Na(42)	0.6013	− 0.1919	0.0516
O(1)	0.1951	0.1759	− 0.3561	O(11)	0.1899	0.1618	− 0.3642
				O(12)	− 0.2007	− 0.1671	0.3605
O(2)	− 0.3769	0.3242	0.2926	O(21)	− 0.3784	0.3170	0.2882
				O(22)	0.3876	− 0.3224	− 0.2974
O(3)	− 0.3566	0.3069	0.8389	O(31)	− 0.3535	0.3074	0.8340
				O(32)	0.3615	− 0.3118	− 0.8359
O(4)	− 0.0759	0.2998	0.1520	O(41)	− 0.0702	0.3093	0.1622
				O(21)	0.0779	− 0.2951	− 0.1476

[a] The barycenter of Co atoms is chosen as the origin.

The refined parameters were determined thanks to the D2b diagram which is the richest in information.

Taking the lattice parameters obtained with X-ray diffraction, and the atomic positions of Na_4CrO_4 as starting points, refinements have been undertaken in the space group $P-1$. This choice is supported by the above discussion and the Mössbauer spectroscopy data which unambiguously show that there is only one iron crystallographic site in the paramagnetic state of Na_4FeO_4 (see below). Furthermore, it may be noted that fits conducted in the $P1$ group do not improve the reliability factor.

The reliability factors for points with Bragg contributions (18) are:

D1b: $N - P + C = 231$, $R_p(\%) = 2.70$, $R_{wp}(\%) = 3.98$, $R_{exp}(\%) = 0.43$, Bragg R-factor $(\%) = 11.1$.

D2b: $N - P + C = 2351$, $R_p(\%) = 4.85$, $R_{wp}(\%) = 6.58$, $R_{exp}(\%) = 2.89$, Bragg R-factor $(\%) = 12.7$.

The observed and calculated diffraction patterns are drawn in Fig. 3. The corresponding crystallographic results, atomic coordinates and selected bond distances and angles are listed in Tables 4, 5, and 6, respectively.

A projection of the structure along [100] is presented in Fig. 4. Table 6 indicates that the FeO_4 tetrahedra are slightly distorted, the value of the mean bond length $\overline{Fe–O} = 1.804$ Å being logically between $\overline{Cr–O} = 1.76$ Å and $\overline{Co–O} = 1.81$ Å, observed in Na_4CrO_4 and Na_4CoO_4, respectively. Four or five oxygen atoms coordinate the four sodium ions at mean distances of 2.33, 2.37, 2.39 and 2.43 Å, respectively.

Among the few iron oxides containing Fe^{4+} high-spin ions actually known, most of them derive from the K_2NiF_4 structure (24). In this structural type, Fe^{4+} (Jahn–Teller ion) is in an elongated octahedron with $Fe–O_{equatorial} = 1.78$ Å and $Fe–O_{axial} = 2.25$ Å. The present compound is the first example of Fe^{4+} high-spin ion in a tetrahedral site. In Table 7, one can appreciate the evolution of the length of the $\overline{Fe–O}$ bond as a function of the oxidation state (x) of tetrahedral iron, which gradually decreases when x increases.

MAGNETISM

Susceptibility Measurements

The thermal variation of χ and $1/\chi$ are presented in Fig. 5. Na_4FeO_4 orders antiferromagnetically below $T_N = 16$ K. In the paramagnetic state, the Curie–Weiss law is obeyed and the effective magnetic moment $\mu_{eff} = 4.9\ \mu_B$ ($C_M = 3.0$ emu/mol) has exactly the value expected for a spin-only Fe^{4+} ($3d^4$) in the high-spin ground state.

The Curie–Weiss temperature is negative ($\theta_P \approx -37$ K) suggesting the occurrence of dominant antiferromagnetic interactions in this compound.

Neutron Diffraction Study

Neutron diffraction patterns have been collected at 25 and 2 K with the D1b spectrometer, namely above and below T_N (Fig. 6).

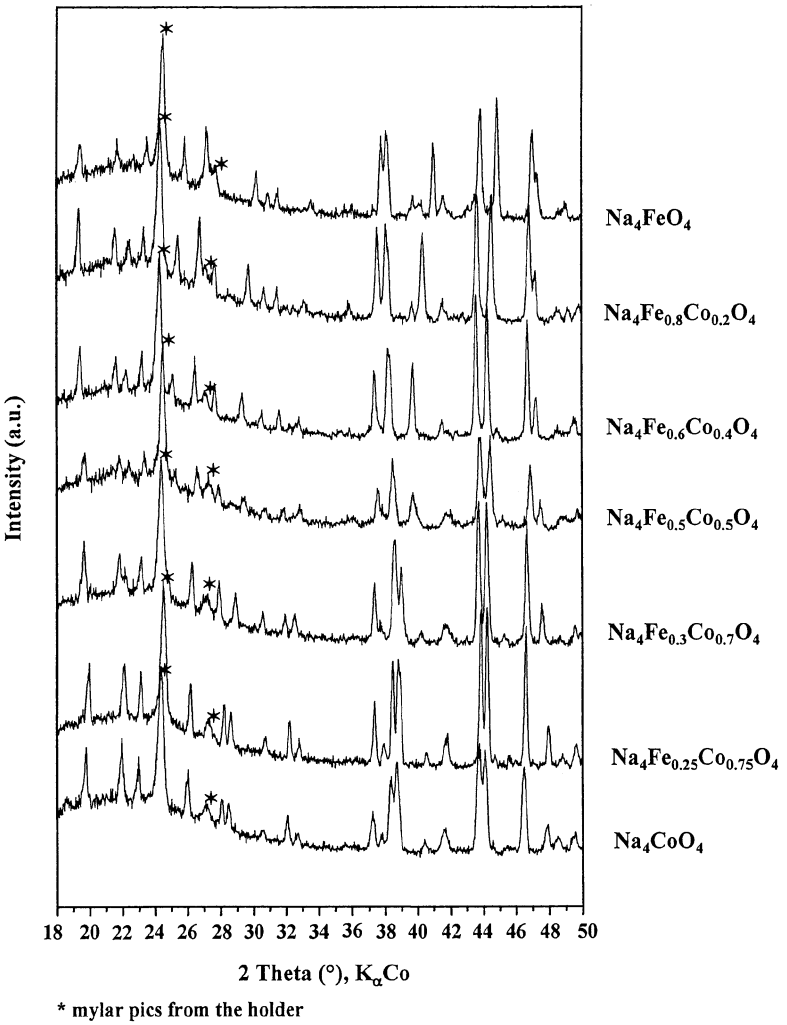

FIG. 2. X-ray powder diffraction patterns for solid solution $Na_4Fe_xCo_{1-x}O_4$ ($x = 0$–1).

At 25 K, the pattern is characteristic of only nuclear scattering and confirms unambiguously the crystal structure deduced from the room temperature X-ray study. The reliability factors for points with Bragg contributions are:

$$N - P + C = 220, \quad R_p(\%) = 1.35, \quad R_{wp}(\%) = 1.89,$$

$$R_{exp}(\%) = 0.839, \quad \text{Bragg } R\text{-factor } (\%) = 6.22.$$

TABLE 3
Lattice Parameters of the $Na_4Fe_xCO_{1-x}O_4$ Solid Solution Phases Measured from Guinier Films

	a (Å)	b (Å)	c (Å)	α (°)	β (°)	γ (°)
Na_4CoO_4	8.64	5.70	6.40	123.9	98.1	99.2
$Na_4Fe_{0.25}Co_{0.75}O_4$	8.61	5.70	6.41	123.9	98.1	99.2
$Na_4Fe_{0.30}Co_{0.70}O_4$	8.60	5.72	6.43	124.2	98.1	100.1
$Na_4Fe_{0.60}Co_{0.40}O_4$	8.55	5.73	6.48	124.3	98.3	101.0
$Na_4Fe_{0.80}Co_{0.20}O_4$	8.51	5.75	6.52	124.5	98.6	101.5
Na_4FeO_4	8.48	5.76	6.56	124.7	98.9	101.8

Note. Uncertainty: ± 0.01 Å and $\pm 0.1°$.

At 2 K, additional lines of magnetic ordering appear which, in agreement with the magnetic measurements, must be antiferromagnetic. These magnetic reflections are indexed with the wave propagation vector $k = (0, \frac{1}{2}, 0)$ (i.e., a doubling of the b-axis of the chemical cell). It should be noted that, due to the strong convolutions between most of the magnetic and nuclear lines, refinements have been carried out using the set of nuclear parameters refined at 25 K and by refining only the scale factor and the magnetic moment components along the three axes of the magnetic cell.

Only two colinear models of magnetic structure are possible and one of them leads to suitable reliability factors

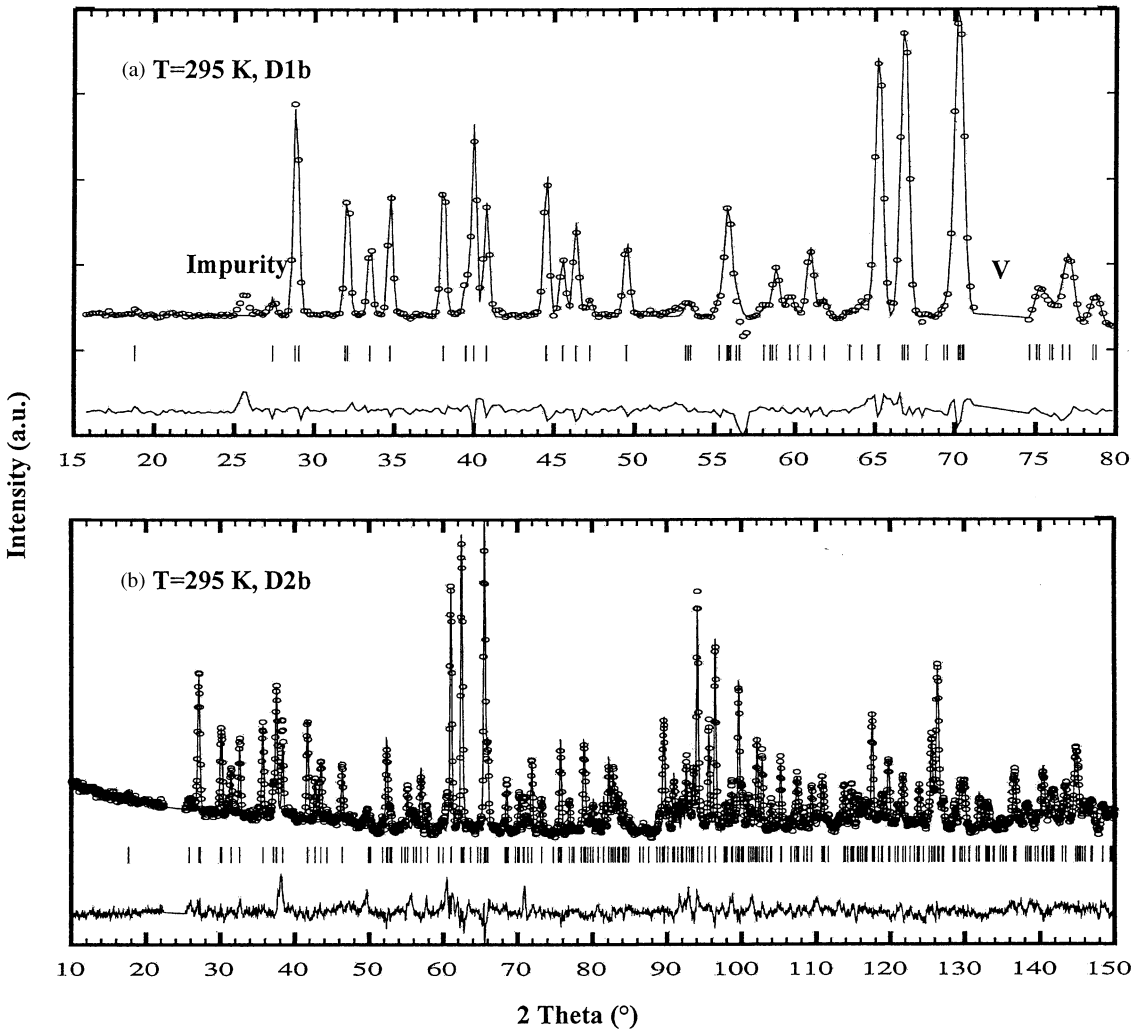

FIG. 3. The observed (circles) and calculated intensities (continuous line) of the neutron diffraction patterns of Na_4FeO_4 recorded at 295 K on: (a) D1b ($\lambda = 2.524$ Å); (b) D2b ($\lambda = 2.400$ Å). The line at the bottom represents the difference between the observed and the calculated profile.

which are:

$$N - P + C = 298, \quad R_p(\%) = 1.46, \quad R_{wp}(\%) = 2.10,$$
$$R_{exp}(\%) = 0.554, \quad \text{Bragg } R_N\text{-factor } (\%) = 5.22.$$
$$\text{Bragg } R_{Mag}\text{-factor } (\%) = 14.4.$$

This model is built with ferromagnetic "chemical cells" which are antiferromagnetically coupled along the *b*-axis direction. This magnetic structure is shown in Fig. 7. It can be described as infinite (010) sheets made of double layers of FeO_4 tetrahedra. In each sheet, the iron atoms are ferromagnetically coupled, the sheets being antiferromagnetically coupled along the [010] direction.

The final values of the magnetic components $\mu(\| a) = 3.50(14)\,\mu_B$, $\mu(\| b) = 2.34(19)\,\mu_B$, $\mu(\| c) = 2.55(21)\ \mu_B$ give a total resultant magnetic moment $\mu_{Fe} = 3.36(12)\,\mu_B$.

The shortest Fe–Fe distances are 4.82 and 5.12 Å within the sheets and 4.90 Å between adjacent sheets. Then, there is no evident relationship among the spin direction and the FeO_4 tetrahedra or the nearest-neighbor Fe–Fe distances.

TABLE 4
Crystallographic Data for Na_4FeO_4

Chemical formula	Na_4FeO_4
Formula weight (g/mol)	211.85
Symmetry	Triclinic
Space group	$P-1$
a (Å)	8.4810(2)
b (Å)	5.7688(1)
c (Å)	6.5622(1)
α (°)	124.662(2)
β (°)	98.848(2)
γ (°)	101.761(2)
V (Å^3)	243.5
Z	2
ρ_{calc} (g/cm^3)	2.92

TABLE 5
Atomic Coordinates for Na_4FeO_4

Atom	Site	x	y	z
Fe	2*i*	0.251(1)	0.567(1)	0.842(1)
Na(1)	2*i*	0.568(1)	0.797(2)	0.515(2)
Na(2)	2*i*	0.990(1)	0.049(2)	0.785(2)
Na(3)	2*i*	0.835(1)	0.360(2)	0.588(2)
Na(4)	2*i*	0.365(1)	0.162(2)	0.960(2)
O(1)	2*i*	0.201(1)	0.164(1)	0.640(1)
O(2)	2*i*	0.614(1)	0.327(2)	0.302(2)
O(3)	2*i*	0.671(1)	0.341(1)	0.840(1)
O(4)	2*i*	0.893(1)	0.237(2)	0.135(1)

TABLE 6
Principal Bond Lengths (Å) and Angles (°) for Na_4FeO_4 at 295 K

FeO_4 tetrahedron			
Fe–O(1)	1.806(7)	O(3)–Fe–O(2)	123.6(1)
Fe–O(2)	1.812(16)	O(3)–Fe–O(1)	98.7(1)
Fe–O(3)	1.802(9)	O(3)–Fe–O(4)	106.6(1)
Fe–O(4)	1.794(14)	O(2)–Fe–O(1)	101.9(1)
		O(2)–Fe–O(4)	100.8(1)
		O(1)–Fe–O(4)	127.6(1)
Na(1)–O(1)	2.370(14)	Na(2)–O(1)	2.303(15)
Na(1)–O(2)	2.397(15)	Na(2)–O(1)	2.411(13)
Na(1)–O(2)	2.331(18)	Na(2)–O(4)	2.289(14)
Na(1)–O(3)	2.420(9)	Na(2)–O(4)	2.340(18)
Na(1)–O(3)	2.439(13)		
Na(3)–O(1)	2.410(12)	Na(4)–O(1)	2.341(15)
Na(3)–O(2)	2.332(17)	Na(4)–O(2)	2.387(14)
Na(3)–O(3)	2.352(15)	Na(4)–O(2)	2.393(14)
Na(3)–O(4)	2.398(10)	Na(4)–O(3)	2.497(13)
		Na(4)–O(4)	2.524(14)

Since a three-dimensional network of isolated FeO_4 units connected through NaO_4 and NaO_5 polyhedrons characterizes the structure, one can conclude that the antiferromagnetic long-range magnetic order (AFM-LRO) arises from magnetic dipolar interactions.

Mössbauer Spectroscopy

Mössbauer spectra recorded at 298 K are presented in Fig. 8. For initial molar ratios Na/Fe < 4, the spectra show two phases: β-$NaFeO_2$ + Na_4FeO_4. As an example, for Na/Fe = 3, we obtain the spectrum shown in Fig. 8b. These results are in fair agreement with the X-ray diffraction analysis.

For Na/Fe = 4 sample (Fig. 8a), one observes a symmetric and well-resolved doublet. It is well fitted by means of one quadrupolar doublet with the following parameters:

$\delta = -0.218 \pm 0.005$ mm/s (isomer shift),

$\Delta = 0.407 \pm 0.005$ mm/s (quadrupolar splitting),

$\Gamma = 0.30 \pm 0.01$ mm/s (linewidth at half-height ($\Gamma_{\alpha Fe\ standard} = 0.27$ mm/s)).

The single doublet is consistent with the space group $P-1$ where only one crystallographic iron site occurs and thus supports the hypothesis made during the crystal structure determination.

The isomer shift value of -0.218 mm/s is in agreement with those obtained for some Fe(IV) compounds (24) and more particularly with those of $Ba_{0.5}La_{1.5}Li_{0.5}Fe_{0.5}O_4$

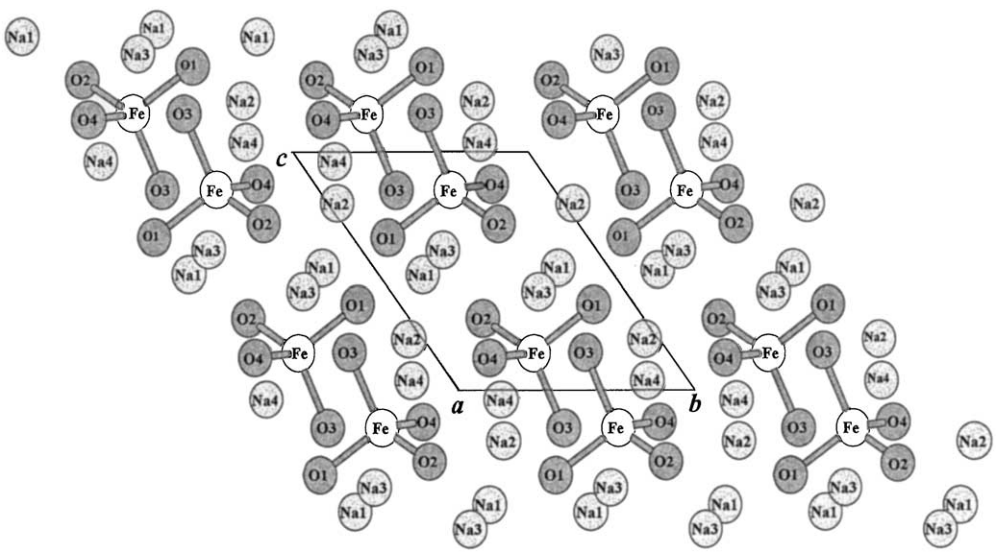

FIG. 4. Projection of the structure of Na_4FeO_4 along [100] showing the FeO_4 tetrahedra.

TABLE 7
Bond Length (Å) for Isolated FeO_4 Tetrahedra in Alkali Ferrates

Oxidation state	Fe^{3+}	Fe^{4+}	Fe^{5+}	Fe^{6+}
Compound	Na_5FeO_4 (27)	Na_4FeO_4 (This work)	NaK_2FeO_4 (26)	Na_2FeO_4 (15)
Fe–O(1)	1.870	1.806	1.69	1.635
Fe–O(2)	1.883	1.812	1.69	1.635
Fe–O(3)	1.901	1.794	1.70	1.643
Fe–O(4)	1.905	1.802	1.70	1.643
Mean $\overline{Fe–O}$	1.89	1.804	1.695	1.64

(− 0.17 mm/s), $Sr_{0.5}La_{1.5}Li_{0.5}Fe_{0.5}O_4$ (− 0.18 mm/s), $Ca_{0.5}La_{1.5}Li_{0.5}Fe_{0.5}O_4$ (− 0.19 mm/s) (25). These compounds crystallize in the K_2NiF_4-type structure where Fe(IV) ions ($t_{2g}^3 e_g^1$) are in distorted octahedral sites. The elongation of the FeO_6 unit stabilizes the high-spin ground state and explains the large quadrupolar splitting observed (1.10–1.27 mm/s at room temperature).

In contrast, the quadrupolar splitting observed in Na_4FeO_4 is smaller (0.41 mm/s) because the coordinence is tetrahedral and distorted.

It is noteworthy that, to our knowledge, it is the first time that the hyperfine parameters of Fe^{4+} ion ($e^2 t^2$) are given (Table 8).

The thermal evolution of the Mössbauer spectra between 295 and 8 K are shown in Fig. 9. A transition to a magnetically ordered state is observed below 15 K, in agreement with the previous magnetization and neutron diffraction measurements.

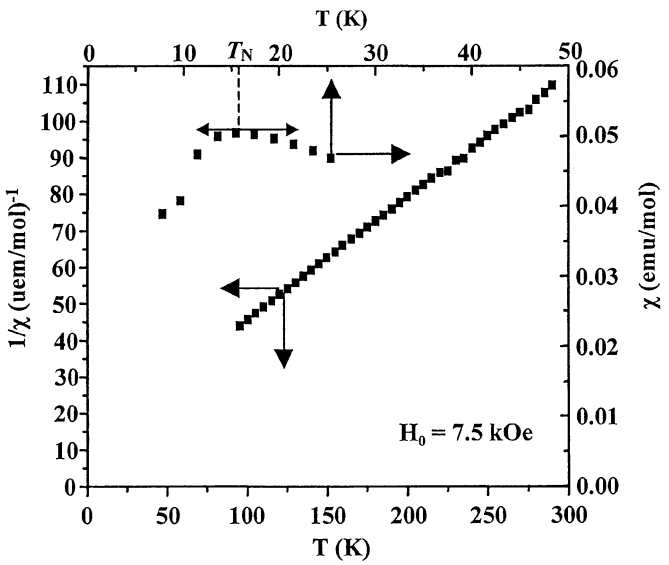

FIG. 5. Temperature dependence of the inverse magnetic susceptibility (Curie law is obeyed) and of the susceptibility ($T_N = 16$ K) of Na_4FeO_4.

At 8 K, the spectrum clearly exhibits a single magnetic hyperfine sextet (once again in fair agreement with the $P - 1$ symmetry). The hyperfine parameters are given in Table 8. We observe a classical increase of the isomer shift and quadrupolar splitting parameters with decreasing temperature. The hyperfine field is reduced (26.24 T) compared with the value expected for an iron ion carrying 4 μ_B. This is probably due to the fact that saturation is not completely reached at 8 K ($T_N = 16$ K).

CHEMICAL REACTIVITY

Chemical Reactivity in Water

Na_4FeO_4 is soluble in water to give a purple coloration, characteristic of the presence of FeO_4^{2-} anion. With the aim of corroborating that Fe^{4+} is disproportionated in solution in Fe^{6+} and Fe^{3+}, we have recorded spectra of $Na_4Fe^{IV}O_4$ and $K_2Fe^{VI}O_4$ solutions with the visible spectrometer "Jeanways 6400" (Fig. 10).

The two spectra exhibit one broad band between 400 and 600 nm, with a maximum near 500 nm, characteristic of FeO_4^{2-} anion. The disproportionation reaction is instantaneous and according to the following equation:

$$3Na_4FeO_4 + 8H_2O \rightarrow 12Na^+ + FeO_4^{2-} + 2Fe(OH)_3 + 10OH^-.$$

Such a behavior has been previously reported for Na_4FeO_4 (9) and Na_2FeO_3 (10), respectively. For this latter compound, Kiselev *et al.* (11) do not agree and claim that "Na_2FeO_3 is soluble in alkalis (NaOH) to give colorless iron-containing solutions".

The absorbance rapidly decreases because FeO_4^{2-} oxidizes H_2O as follows:

$$2FeO_4^{2-} + 5H_2O \rightarrow 2Fe(OH)_3 + 3/2O_2 + 4OH^-.$$

The complete hydrolyze of Na_4FeO_4, takes, at the very most, 30 min whereas, in the same conditions, the reduction of K_2FeO_4 is over after sever hours.

Study of the Decomposition of Na_4FeO_4 by Mössbauer Spectroscopy

As already mentioned, Na_4FeO_4 is highly hygroscopic and we have followed this behavior by Mössbauer spectroscopy.

The absorber is made of a finely ground sample placed between two "Scotch" sheets that are permeable to atmospheric humidity. The sample is placed, at $T = 295$ K, on the spectrometer during 48 h and the data are read successively after 6, 12, 24, 36, and 48 h. So we have obtained the five spectra shown in Fig. 11.

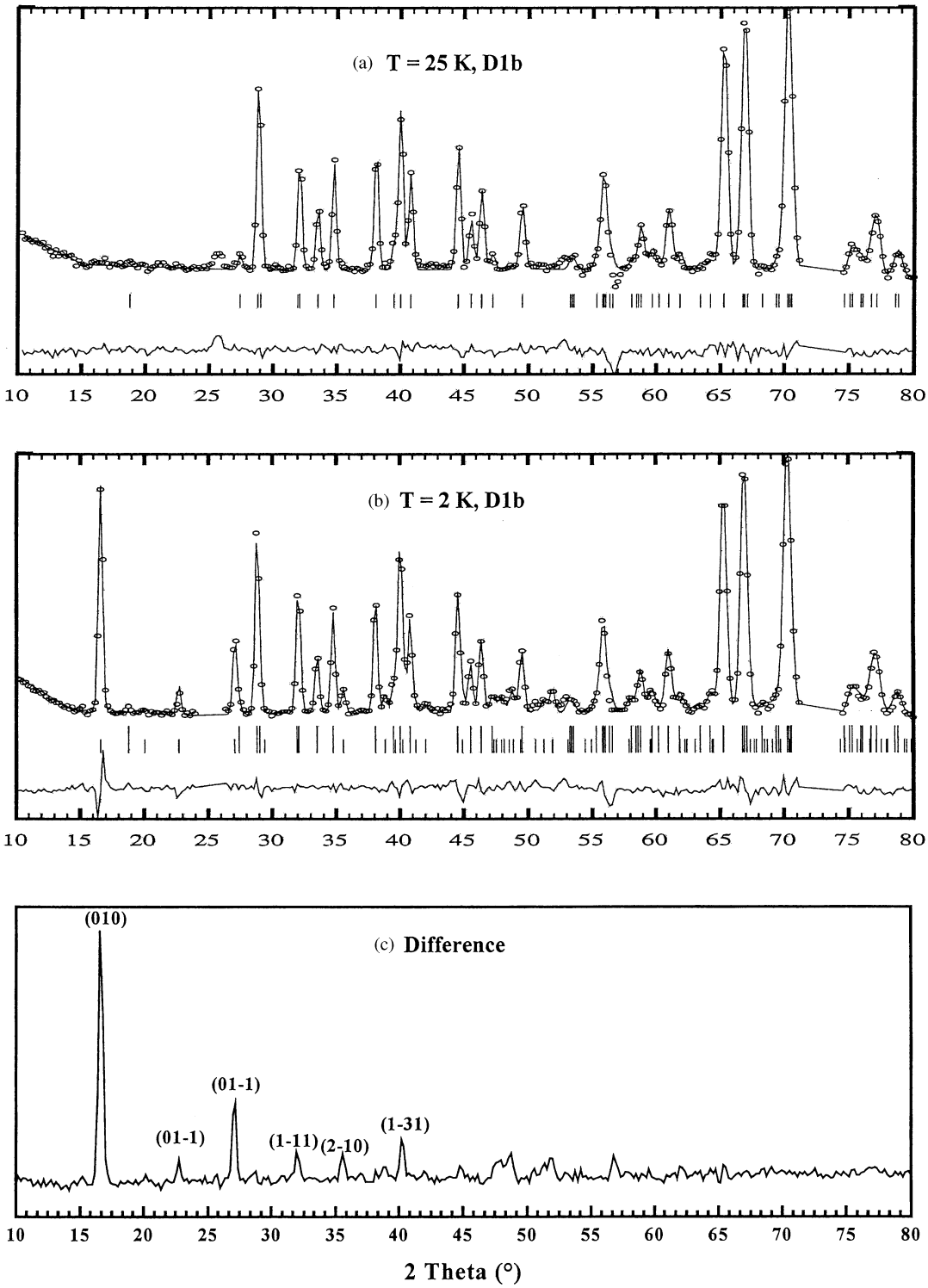

FIG. 6. Observed (points) and calculated neutron powder diffraction profile (continuous line) of Na_4FeO_4 recorded on D1b: (a) $T = 25\,K$; (b) $T = 2\,K$; (c) difference profile between the observed spectra (indexation in the magnetic cell: $a_{mag} = a_n$, $b_{mag} = 2b_n$, $c_{mag} = c_n$).

They are fitted with different quadrupolar doublets and/or single line that are associated with phases of different isomer shifts. These results allow to follow the evolution of the hydrolyze reaction and to characterize the intermediate products.

(1) After 6 h—one phase and one oxidation state:

$\delta = -0.22$ mm/s, $\Delta = 0.41$ mm/s, $\Gamma = 0.30$ mm/s:

doublet assigned to Na_4FeO_4.

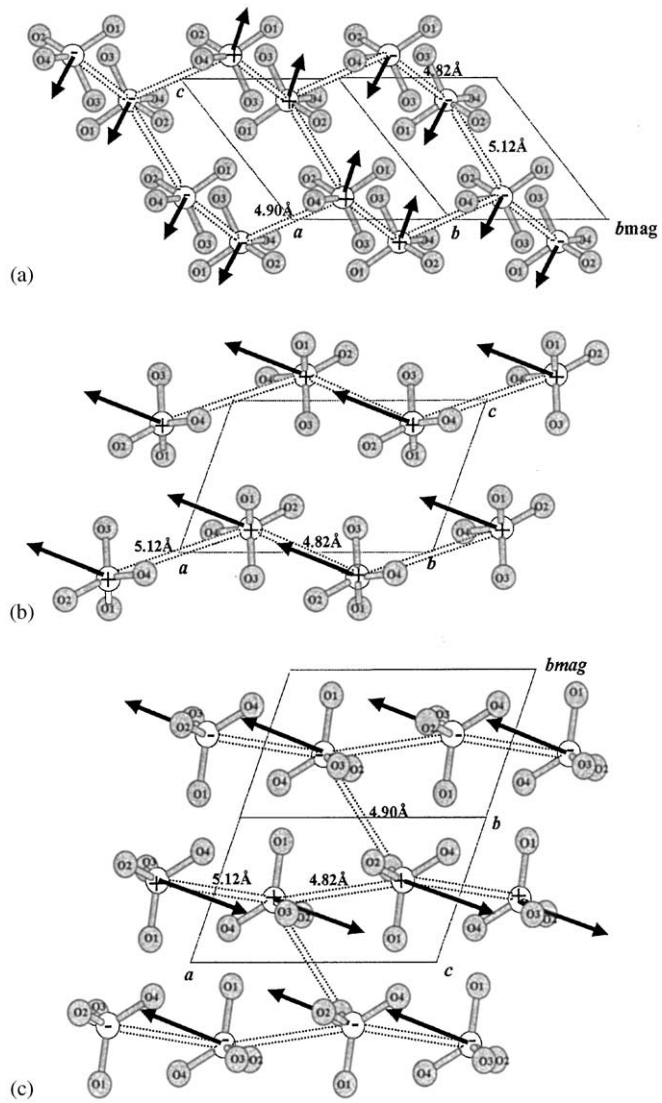

FIG. 7. Projections of the collinear magnetic structure of Na_4FeO_4 along [100], [010], and [001] showing the magnetic moment direction. The Na atoms are omitted.

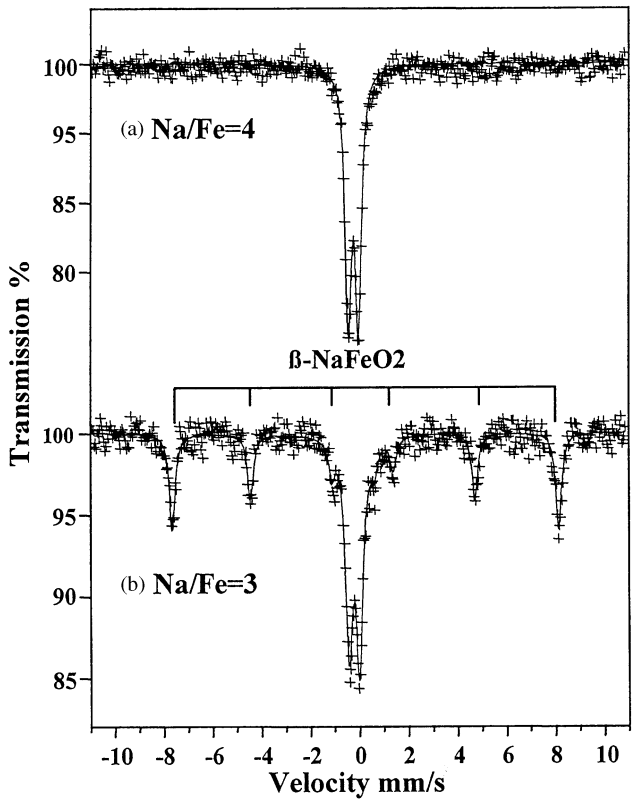

FIG. 8. Mössbauer spectra of Na_4FeO_4 (2a) and $Na_4FeO_4 + \beta$-$NaFeO_2$ (2b) at 295 K.

(2) After 12 h—three phases and three oxidation states:

$\delta = -0.22$ mm/s, $\Delta = 0.41$ mm/s, $\Gamma = 0.31$ mm/s,

$I = 36\%$: doublet assigned to Na_4FeO_4,

$\delta = -0.83$ mm/s, $\Delta = 0$ mm/s, $\Gamma = 0.31$ mm/s,

$I = 12\%$: single line assigned to Na_2FeO_4,

$\delta = 0.41$ mm/s, $\Delta = 0.33$ mm/s, $\Gamma = 0.47$ mm/s,

$I = 52\%$: doublet assigned to FeO(OH).

Fe^{4+} is still present ($\delta = -0.22$ mm/s) at $\approx 30\%$, and 70% is disproportionated in Fe^{6+} ($\delta = -0.83$ mm/s) and Fe^{3+} ($\delta = 0.41$ mm/s) according to the equation: $3Fe^{4+} \rightarrow 1Fe^{6+} + 2Fe^{3+}$. The Fe^{3+}/Fe^{6+} ratio is greater than 2, so this shows that Fe^{6+} is reduced by atmospheric moisture.

(3) After 24 h—two phases and two oxidation states:

$\delta = -0.83$ mm/s, $\Delta = 0$ mm/s, $\Gamma = 0.27$ mm/s, $I = 14\%$:

single line assigned to Na_2FeO_4,

$\delta = +0.36$ mm/s, $\Delta = 0.31$ mm/s, $\Gamma = 0.38$ mm/s,

$I = 86\%$: doublet assigned to FeO(OH).

TABLE 8
Mössbauer Parameters for Na_4FeO_4

T (K)	δ^a (mm/s)	Δ (mm/s)	2ε (mm/s)	H (T)	Γ (mm/s)
295	−0.218	0.407			0.30
25	−0.130	0.440			0.30
6	−0.140		0.205	26.24	0.28

[a] Relative to room temperature α-iron foil $\delta \pm 0.005$, $\Delta \pm 0.005$, $2\varepsilon \pm 0.005$, $H \pm 0.01$

$$\Delta = \frac{eQV_{ZZ}}{2}\left(\frac{1+\eta^2}{3}\right)^{1/2}$$

$$2\varepsilon = \frac{eQV_{ZZ}}{2}\left(\frac{3\cos^2\theta - 1 + \eta\sin^2\theta\cos 2\varphi}{2}\right).$$

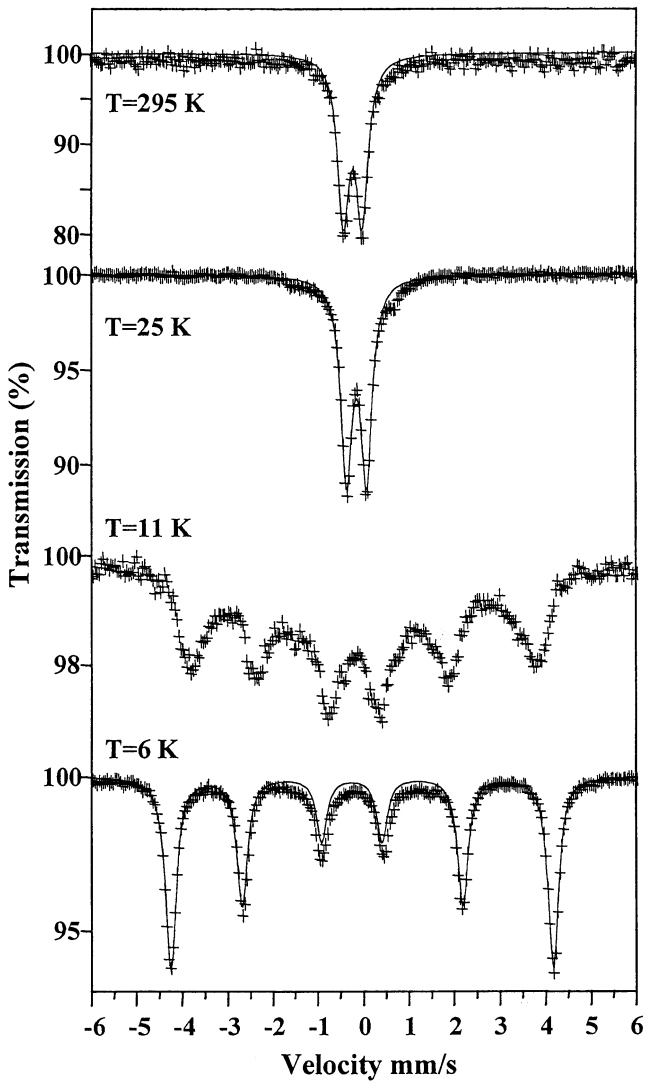

FIG. 9. Mössbauer spectra of Na_4FeO_4 at 295, 25, 11 and 6 K.

The Fe^{4+} doublet disappears completely, Fe^{6+} is still present, the quadrupolar splitting of the Fe^{3+} doublet is relatively small.

(4) After 36 h—three phases and two oxidation states:

$\delta = -0.85$ mm/s, $\Delta = 0$ mm/s, $\Gamma = 0.49$ mm/s, $I = 3\%$:

single line assigned to Na_2FeO_4,

$\delta = +0.31$ mm/s, $\Delta = 0.44$ mm/s, $\Gamma = 0.41$ mm/s,

$I = 53\%$: doublet assigned to FeO(OH),

$\delta = 0.33$ mm/s, $\Delta = 0.79$ mm/s, $\Gamma = 0.41$ mm/s,

$I = 44\%$: doublet assigned to FeO(OH).

The Fe^{6+} single line has almost completely disappeared; therefore all Fe^{6+} ions are reduced in Fe^{3+}. We have chosen to fit the Fe^{3+} spectra with two doublets with large line width that represent ferric oxyhydroxide of badly defined morphology.

(5) After 48 h—two phases and one oxidation state:

$\delta = 0.31$ mm/s, $\Delta = 0.57$ mm/s, $\Gamma = 0.36$ mm/s,

$I = 54\%$: doublet assigned to FeO(OH),

$\delta = +0.35$ mm/s, $\Delta = 0.68$ mm/s, $\Gamma = 0.36$ mm/s,

$I = 46\%$: doublet assigned to FeO(OH).

Between 36 and 48 h, the hydrolysis of Fe^{3+} progress and the asymmetric final doublet is ascribed to amorphous $Fe(OH)_3$ or FeO(OH). The parameters $\delta = 0.31$ and 0.35 mm/s, $\Delta = 0.57$ and 0.68 mm/s characterize Fe^{3+} ion in distorted octahedral sites like in goethite or lépidocrocite. At this stage, the absorber is rust colored and does not diffract X ray.

CONCLUSION

Pure Na_4FeO_4 was synthesized for the first time at 400°C, by solid-state reaction between Na_2O_2 and $Fe_{1-x}O$.

This compound belongs to the Na_4MO_4 (M = Ti, Cr, Mn and Ge, Sn, Pb) phases, which crystallize in the triclinic system ($P-1$). Fe atoms occupy slightly distorted tetrahedrons with a mean distance Fe–O of 1.80 Å. ^{57}Fe Mössbauer effect shows that Fe is in the high-spin Fe^{4+} state: d^4 (e^2t^2). It is the first time (to our knowledge) that this Fe^{4+} state is fully characterized: $\delta = -0.22$ mm/s $\Delta = 0.41$ mm/s at room temperature.

Na_4FeO_4 is antiferromagnetic below $T_N = 16$ K. The magnetic structure is collinear with a magnetic moment of 3.36 μ_B per iron ion.

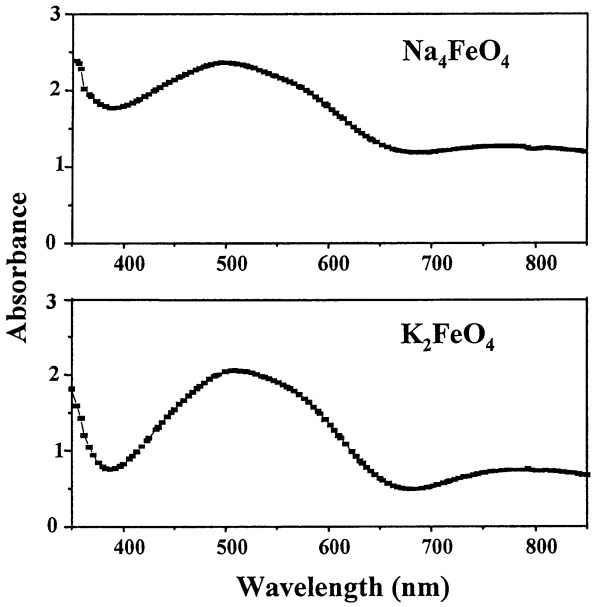

FIG. 10. Visible spectra of Na_4FeO_4 and K_2FeO_4.

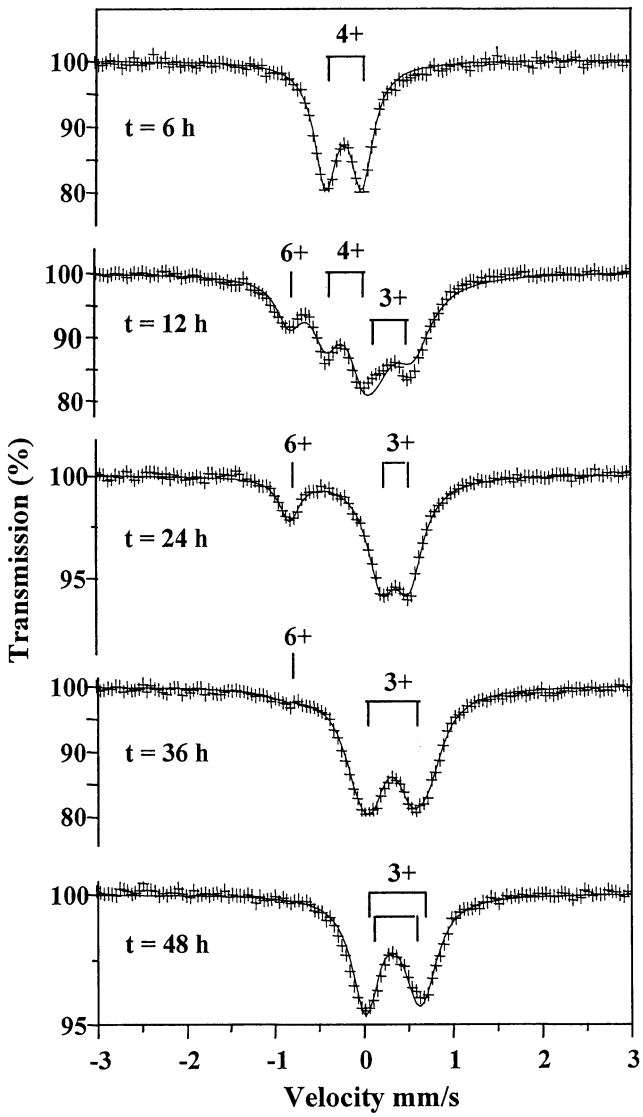

FIG. 11. Mössbauer spectra of Na_4FeO_4 recorded at 295 K, successively after 6, 12, 24, 36 and 48 h (see text).

Na_4FeO_4 is neither stable in water nor on contact with atmospheric moisture. In both cases, we have shown that it is disproportionated in Fe^{3+} and Fe^{6+}.

REFERENCES

1. H. Rieck and R. Hoppe, *Naturwissenschaften* **61**(3), 126 (1974).
2. A. El Balkhi, M. Zanne, C. Gleitzer, and A. Courtois, *J. Sol. State Chem.* **19,** 293 (1976).
3. C. Romers, C. J. M. Rooymans, and R. A. De Graaf, *Acta Crystallogr.* **22,** 766 (1967).
4. J. Thery and R. Collongues, *Compt. Rend.* **247,** 2003 (1958).
5. T. Birchall, N. N. Greenwood, and A. F. Reid, *J. Chem. Soc.* (*A*) **3,** 2383 (1969).
6. G. Brachtel and R. Hoppe, *Naturwissenschaften* **64,** 271 (1977).
7. A. Tschudy and H. Kessler, *Compt. Rend, Acad. Sci.* **273C,** 1435 (1971).
8. Y. Takeda, K. Nakahara, M. Nishijima, N. Imanishi, O. Yamamoto, and M. Takano, *Mater. Res. Bull.* **29**(6), 659 (1994).
9. R. Scholder, Hv Bunsen, and W. Zeiss, *Z. Anorg. Allg. Chem.* **283,** 330 (1956).
10. J. R. Harrison and C. Toole, U.S. Patent 2,835,553 (1958).
11. Yu. M. Kiselev, N. S. Kopelev, and Yu. D. Pervil'ev, *Russ. J. Inorg. Chem.* **32**(12), 1729 (1987).
12. R. Scholder, *Bull. Soc. Chim. Fr.* **7,** 1112 (1965).
13. U. Croatto, *La Ricerca Scientifica*, **19,** 1007 (1949).
14. Yu. M. Kiselev, N. S. Kopelev, N. A. Zav'yalova, and Yu. D. Pervil'ev, *Russ. J. Inorg Chem.* **34**(9), 1250 (1989).
15. G. Malchus and M. Jansen, *Z. Anorg. Allg. Chem.* **624,** 1846 (1998).
16. N. S. Kopelev, *ln* "Mössbauer spectroscopy of sophisticated oxides." (A. Vértes and Z. Homonnay, Eds.), p. 305, Akadímiai Kiadó, Budapest, Hungary, 1996.
17. H. M. Rietveld, *J. Appl. Crystallogr. Sect. C* **52,** 762 (1996).
18. J. Rodriguez-Carjaval, *Physica B* **192,** 65 (1993).
19. Le Caer, private communication.
20. R. Olazcuaga, J. M. Reau, M. Devalette, G. Le Flem, and P. Hagenmuller, *J. Solid State Chem.* **13,** 275 (1975).
21. J. Kissel and R. Hoppe, *Z. Anorg. Allg. Chem.* **582,** 103 (1990).
22. R. Hoppe and W. Scheld, *Z. Anorg. Allg. Chem.* **546,** 137 (1987).
23. M. Jansen, *Z. Anorg. Allg. Chem.* **417,** 35 (1975).
24. F. Menil, *J. Phys. Chem. Solids* **46,** 153 (1985).
25. G. Demazeau, N. Chevreau, L. Fournes, J. L. Soubeyroux, Y. Takeda, M. Thomas, and M. Pouchard, *Rev. Chim. Min.* **20,** 155 (1983).
26. C. Jeannot, B. Malaman, and R. Gérardin, Univ. thesis, Nancy, France, 2000.
27. G. Brachtel and R. Hoppe, *Z. Anorg Allg. Chem.* **446,** 77 (1978).